et al /J. Pharm. Sci. & Res. Vol. 12(1), 2020, 31-36

ISSN:0975-1459
Journal of Pharmaceutical Sciences and Research
www.jpsr.pharmainfo.in

PLA/PEG scaffolds for Tissue Engineering applications: In-Vitro cytocompatibility

Abstract:

An ideal tissue engineering scaffold material should be biodegradable, biocompatible, and also must possess adequate mechanical strength. The aim of this work is to develop Poly-lactic acid and Poly-ethylene glycol (PLA-PEG) composite scaffolds with varied weight ratios of polymers to meet the essential characteristic features of scaffold used in tissue engineering. These scaffolds were prepared using the solvent casting-particulate leaching technique and characterized with respect to pore size, mechanical strength, in-vitro degradation, and cytocompatibility of Human Mesenchymal stem cells (hMSC's). We have observed that the increased PEG content in the composite scaffold increases the degradation rate, and also larger pores formed. All the scaffolds were exhibited the pore size in the range of 224-327 µm. The metabolic activity of hMSC's on scaffolds results indicated that all the scaffolds are cytocompatible. The cell attachment on the scaffolds also displayed, which proved that cells are well compatible and adhere to the scaffolds. In summary, the results directed to continue further studies to specific tissue engineering applications, especially the mechanical strength and pore size of the scaffold had met the bone tissue requirements.

Keywords: PLA, PEG, solvent casting-particulate leaching technique, mechanical strength, cytocompatibility.

1. INTRODUCTION:

Biomaterials play a pivotal role in tissue engineering and regenerative medicine, where they provide biophysical and biochemical stimuli to guide cells for tissue formation in a Spatio-temporal fashion, and also facilitate the structural and functional restoration of damaged tissues, both in cellular and acellular therapies (Place et al. 2009). Biomaterials should provide a three-dimensional porous structural support (3D) to aid the cellular interactions to regulate the behavior and function, and also attain mechanical strength along with active mass transport in arbitrary and complex 3D structures (Sultana and Wang 2012). Synthetic materials have been widely used in tissue engineering and regenerative medicine. The scaffolding materials such as polyurethane (PU) (Guelcher 2008), poly(ϵ-caprolactone) (PCL), poly(lactic acid-co-glycolic acid) (PLGA) (Kumar Mekala et al. 2013), poly(lactic acid) (PLA)-poly(ethylene glycol) (PEG) co-block polymers (Serra et al. 2014), cholesterol-PEG-poly(D,L-lactic acid) copolymers (Yu et al. 2006), polylactide/cross-linked polyurethane (PLA/CPU) (Liu et al. 2014), poly(L-lactic acid)/β-tricalcium phosphate (Liu et al. 2013) are widely tested for tissue engineering and regenerative medicine. PLA is biodegradable, biocompatible, and readily susceptible to modifications. However, the hydrophobic nature of PLA restricts its usage in tissue Engineering applications. This disadvantage of PLA can be subsided and rectified by modifying the physicochemical properties of PLA by adding a hydrophilic polymer. Poly (ethylene glycol) (PEG) is a crystalline, hydrophilic polymer, which is well known for its non-toxic and biocompatibility (Chen et al. 2015). PEG is introduced into the PLA not only to increase its hydrophilicity but also to assist controllable degradation (Chiu et al. 2010). However, up to our knowledge in detail, exploration of synthetic polymers like PLA and PEG as a composite scaffold is limited in tissue engineering applications.

Various methodologies such as supercritical CO_2 gas foaming and particle leaching, emulsion freezing/freeze-drying, and solvent casting-particulate leaching have been used for developing porous scaffold (Sultana and Wang 2012, Chen et al. 2015, and Murphy et al. 2002). The solvent casting-particulate leaching technique is widely accepted, incorporating the interconnected hierarchical porosity in the scaffold, making nutrient transport and waste elimination easier (Chiu et al. 2010).

In the previous study, we tested PLA-PEG scaffolds for bone matrix deposition using MLO-A5 cells. However, the detailed study of the mechanical properties and degradation behavior were not covered. In the present study, PLA-PEG composite scaffolds characterized them for physicochemical, and mechanical properties. Apart from that, biodegradation and biocompatibility tests were performed to evaluate their role as a potential biomaterial.

2. EXPERIMENTAL

Materials

PLA4042D procured from Natureworks®, Polyethylene glycol (PEG4000) (Sigma). Both the polymers were vacuum dried for 24 hrs prior use. Dichloromethane was used as a solvent and purchased from HIMEDIA. DMEM-Dulbecco's Modified Eagle's medium, FBS-Fetal bovine serum (FBS), PBS-Phosphate buffer saline, and Penicillin have been used for cell culture study, obtained from Invitrogen. MTT-5-dimethylthiazol-2-y1]-2, 5-diphenyl tetrazolium bromide for cytocompatibility and cell fixing agent glutaraldehyde and Dimethyl Sulphoxide were procured from Sigma Aldrich Chemicals.

Preparation of PLA-PEG Scaffolds

Solvent casting-particulate leaching technique used for scaffold fabrication, here NaCl used as a particulate porogen (300-400 µm) (Sah and Pramanik 2014). Different weight ratios 90:10, 85:15, 80:20, and 75:25 of PLA and PEG were taken and dissolved in dichloromethane by stirring them overnight. This polymer

solution was poured slowly at the edge of Petri-dishes containing porogen in the weight/weight ratio of 1:9. Then, polymer blends were vacuum dried for 48 hrs to evaporate the solvent. Scaffolds were immersed in de-ionized water for 2-3 days (fresh water was added for every six hours) to leach out NaCl which helps in the construction of porous scaffold. The prepared scaffolds were cut into a circular disc (1 cm diameter).

CHARACTERIZATION

Morphological Analysis (SEM). Scanning Electron Microscope - SEM (S-3700N Hitachi) was used to evaluate the morphology and determine the pore size of developed PLA-PEG composite scaffolds. Before imaging, samples were vacuum dried for 60 min at 45°C, followed by Gold sputter (Hitachi, E1010) coating. The pore size of the prepared scaffolds was analyzed by the Image-J software.

Phase Analysis (XRD). X-ray diffraction measurements were performed using an XRD 7000 X-ray (7000, Shimadzu) diffractometer with CuKα radiation (λ = 1.542 Å). The machine operated at 40 kV and 30 mA. X-ray diffractograms of the samples have been recorded with a scan rate of 2°/min and in the 2θ range of 10°–80°

Structural Analysis (FT-IR). Fourier Transform Infrared Spectra of the prepared composite scaffolds were obtained using a Fourier Transform Infrared spectrophotometer (8400S, Shimadzu) were collected between 500 and 4000 cm^{-1} frequency range. 400 mg of Potassium Bromide (Kbr) was used to pelletize the samples by using a hydraulic press. The spectra obtained when the machine was allowed to run in transmittance mode within a range of 500 to 4000 cm^{-1}.

Thermal Analysis (DSC). Thermal behavior of the scaffolds was studied using differential scanning calorimeter (DSC-60, Shimadzu)-DSC provided with a liquid nitrogen cooling system. Scaffold samples about 10 mg were placed in sealed aluminum pans, then subjected to heat in a range of 21°C (room temperature) to 300°C at the heating rates of 10°C/min. A baseline correction performed by recording a run with empty pans.

Compressive Moduli. The compressive strength of developed scaffolds with specific dimensions (10 mm dia × 7 mm thick) was measured by using Universal Testing Machine (H10K-S, USA) with a crosshead speed of 1 mm/min, with a load cell of 100 N. The test performed at ambient conditions. $S = F_{max}/A$ was used to calculate the compressive moduli (S) of the sample. F_{max} and A represents applied load and the initial cross-sectional area of the scaffold sample, respectively.

In-vitro Biodegradation. The Simulated body fluid (SBF) containing 500 mg/ml of lysozyme was used to evaluate the degradation of prepared scaffolds according to a published protocol (Kokubo et al. 1990)**.** The initial weight of the sample recorded as Wo. The scaffold samples were immersed in 15 mL of SBF and kept for mild shaking at specific intervals of time (1, 7, 14, 21, 28, 35, and 42 days). The degradation studies were carried out at 37 °C. Scaffolds were collected from SBF at each time point as mentioned above, rinsed with water, and finally weighed after freeze-drying. The final weight recorded as Wt. The leftover weight percentage (WR) was calculated using the formula given below.

$$\% \quad Weight \quad remaining = 100 - [(W_o - W_t)/W_o \times 100]$$

In-vitro Cell Study

Scaffold sterilization, Cell Culture, and Seeding

Umbilical cord blood used as a source for Mesenchymal stem cells (MSCs), and they were cultured medium containing 90% DMEM, 10% FBS, and 1% penicillin solution. The media has been changed for every alternate day, and the cells have been subcultured till the fifth passage (Bissoyi and Pramanik 2013). Sterilization of scaffold samples by using 70% ethanol was performed and washed with PBS. The sterilized scaffolds have been incubated in culture medium for 12 hrs, followed by cell seeding. Finally, cells were seeded on these sterilized scaffolds with a load pay of 5 X 10^5 cells/mL by a static method.

Metabolic activity and Cell attachment

Metabolic activity of cells seeded on scaffolds was investigated by MTT [3-(4,5-dimethyl-thiazol-2-y1)2,5-diphenyltetrazolium bromide] assay based on the published elsewhere (Xu et al. 2010). In brief, ten µL of MTT solution (5 mg/ mL) was added to the culture plate and incubated at 37°C for 4 hrs. 100 µL Dimethyl sulfoxide was used to solubilize the formazan crystals, and the absorbance was recorded using a micro-plate reader (2030 multi-label reader Victor X3, Perklin Elmer, USA) at 595 nm.

Cell spreading and attachment of the seeded cells on the scaffold was observed by SEM at 30 kV using a high vacuum (S-3700N Hitachi). Glutaraldehyde (3% vol/vol) has been used as a fixing agent. Samples were rinsed with wash buffer twice, and a series of ethanol wash was performed, followed by drying (Xu et al. 2004). Cell scaffold constructs were gold sputter-coated (Hitachi, E1010) before imaging.

Statistical Analysis

Graphpad prism 7.0 has been employed for statistical analysis using the student's t-test. The mechanical property, biodegradation, and MTT assay experiments have been conducted in triplicate per each condition (n=3). The probability value less than 0.05 ($p<0.05$) treated as statistical significant.

RESULTS AND DISCUSSION

Development of Scaffolds

PLA-PEG composite scaffolds have been developed by the solvent casting and particle leaching method. The developed scaffolds are denoted as PE90:10, PE85:15, PE80:20, and PE75:25. Here, P and E indicate PLA and PEG polymers, respectively.

Morphological Analysis

Pore size and porosity were the crucial factors for efficient nutrient transport and also aided cell migration (Delaine-Smith et al. 2014). The morphology of PLA-PEG copolymer scaffolds have been examined by using a scanning electron microscope, and the images have been illustrated in **Figure 1.**

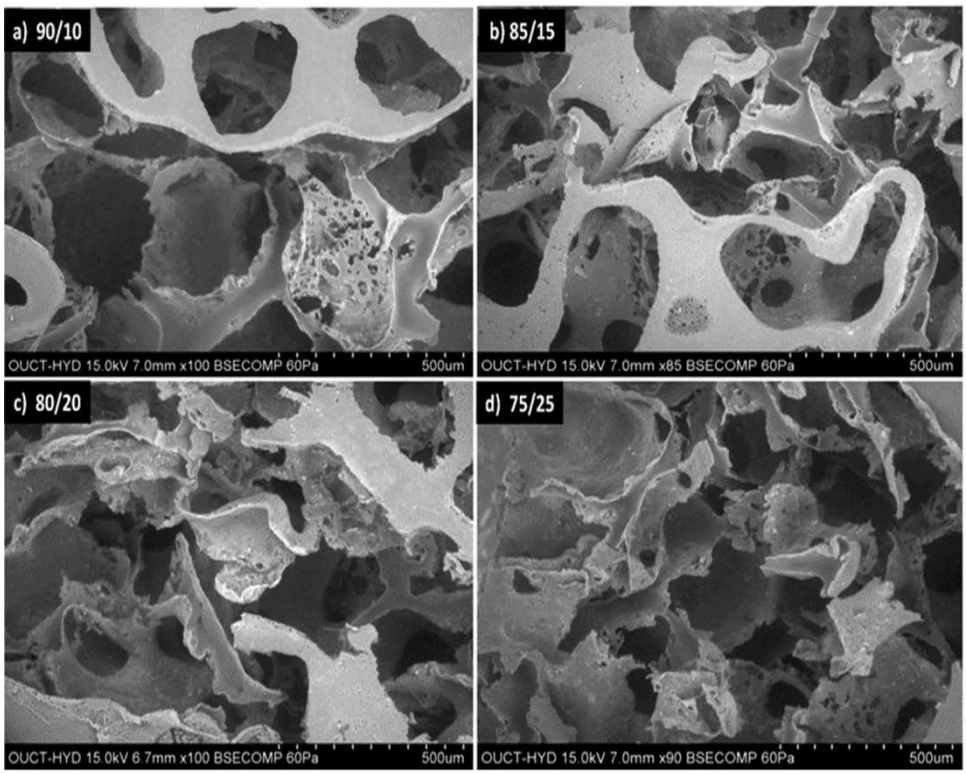

Figure 1: Microscopic images of scaffolds a) PE 90:10; b) PE 85:15; c) PE 80:20; d) PE 75:25

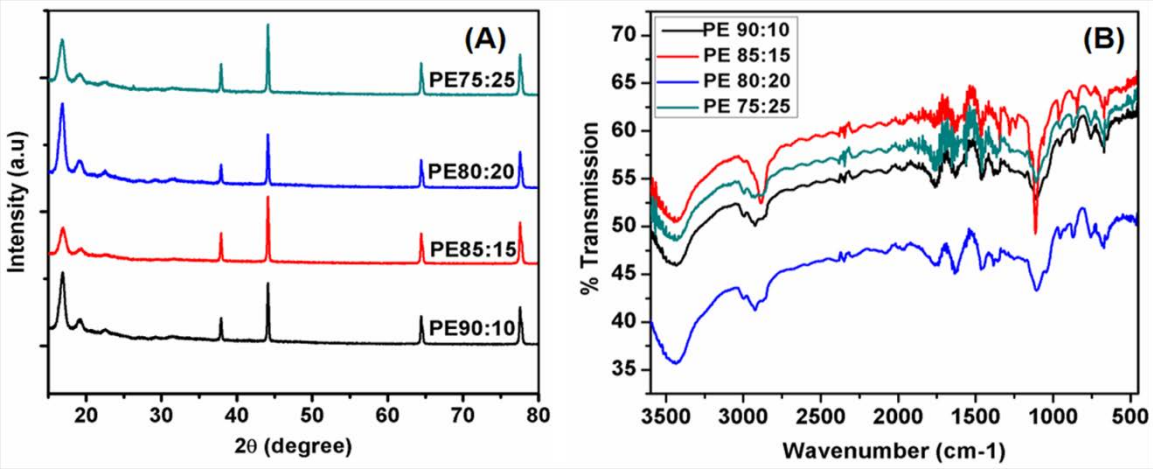

Figure 2: (A) X-ray diffraction (XRD) and (B) Fourier transform infrared (FT-IR) patterns of composite PLA-PEG scaffolds

The pores have been formed in leached scaffolds irrespective of PEG weight ratio, and the pore size range was 224-327 µm as evaluated with Image J. Further, we noticed an increase in the pore size of scaffolds as PEG content increased and the corresponding ranges are PE 90:10 (224-267 µm), PE 85:15 (245-289 µm), PE 80:20 (248-304 µm), PE 75:25 (255-327 µm). The PEG content could have facilitated pore emergence, which resulted in large pores formation in higher PEG contained scaffolds. The obtained pore size was by porogen used, and this is in the optimal pore size range for bone tissue engineering (Burg et al. 2000).

Phase Analysis

XRD was used to gain information about the phases of composite scaffolds (Padmanabhan et al. 2014). XRD investigated the crystalline structure of synthesized scaffolds and the results were shown in **Figure 2 (A).** The maximum diffraction peak was observed in all composite scaffolds at 2θ=16.8˚ for PLA attributes the crystallinity nature. This diffraction pattern of PLA is consistent with the results reported earlier (Zhu et al. 2015). The peaks at 2θ= 19.3˚ and 23.4˚ were noticed in all the composite scaffolds in **Figure 2 (A)**. The peaks in the diffraction pattern of PEG were reported at 2θ=19.1 ˚ and 23.2˚, which denoted the crystallinity nature of PEG (Wang et al. 2012). The intensity of the peaks have been increased in the diffraction patterns of PLA-PEG scaffolds with an increasing weight ratio of PEG. As shown in **Figure 2 (A),** the diffraction pattern of all composite scaffolds was similar to a change in the intensity of the peaks. The

results are confirming that the crystalline nature of copolymer scaffolds changed due to the addition of PEG to PLA. The results of this study confirmed the crystalline nature of PLA is affected by the addition of PEG and formed the semi crystal polymeric scaffolds. The concentration of PEG in polymer blends affect the degradation behavior, and crystallinity was increased with a higher percentage of PEG in PLA/PEG polymer blends (Serra et al. 2014).

Structural Analysis

The individual components of a composite system and its interactions information has been given by FT-IR analysis (Cai et al. 2009). FT-IR spectra of PLA-PEG composite scaffolds have been depicted in **Figure 2 (B).** The stretching frequencies of PLA for C=O, $–CH_3$, and C–O, appeared at 1514-1755, 3457, and 1096 cm−1, respectively. PLA bending frequencies for $–CH_3$ observed at 1364-1467 cm^{-1}. C=O, C-O, $–CH_3$ stretching frequencies of PEG appeared at 1553-1984, 1096-1459, 2865 cm^{-1}, respectively. A wide-ranging peak has been observed in the range of 3149-3654 cm−1 for PEG, which represents the terminal hydroxyl group. FT-IR spectra of all different combinations of PLA-PEG show similar peaks in all the combinations and also C=O, $–CH_3$, and C–O bending and stretching frequencies of PLA and PEG were noticed in **Figure 2(B).** The stretching and bending frequencies have been taken from reported literature attributes the characteristic features of PLA and PEG (George 2001; Rozenberg et al. 1998; Matsuura et al. 1973; Miyazawa et al. 1962; Zhu et al. 1990).

Thermal Analysis

The melting peaks of all composite scaffolds exhibiting the same behaviour, as illustrated in **Figure 3.** The results of DSC have shown the decomposition temperature decreases with increasing concentration of PEG in PLA-PEG scaffolds. The melting point of composite scaffolds is 154°C. The addition of PEG to PLA has been shown the peak variation in the range of 260-350°C in all scaffolds. The results of the current investigation confirming that the decomposition temperature affected by the weight % of PEG in composite scaffold, and also this makes a notable significance in degradation studies also (Jiang and Liao 2012).

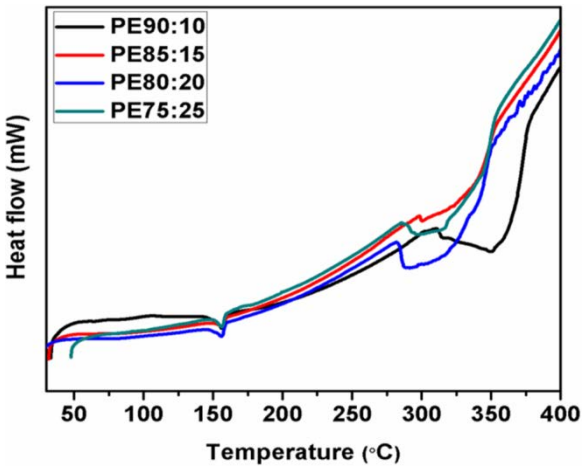

Figure 3: Differential scanning calorimetric thermogram of PLA-PEG composite scaffolds

Mechanical Property

The mechanical property is also one of the key parameters in designing of the scaffold, especially load-bearing tissues such as bone requires higher mechanical strength to resist exerted physical stress (Causa et al. 2006; Lu and Mikos 1996). It's a well-known fact that adding a synthetic polymer will strengthen the mechanical property of porous scaffolds, as observed in the published literature (Siddiqui and Pramanik 2014), we also found in the current study increased compressive moduli of PLA-PEG composite scaffold as depicted in **Figure 4 (A).** The values of composite scaffolds with varied ratios of PLA-PEG as PE90:10 (55.18±1.8MP), PE85:15 (64.42±2.1MPa), PE80:20 (59.34±2.4MPa) and PE75:25 (51.39±1.2Mpa). Compressive moduli of composite scaffolds are shown to increase with a decrease in PEG content up to 15% (85:15), followed by a steep decrease in other composite scaffolds such as 90:10. The obtained values are in the range of compressive moduli of cortical bone 50–200 MPa. In previous reports, the compressive moduli of PLA-PEG composite scaffolds were in the range of 85-207MPa by using smaller particle-sized NaCl crystals (Yin et al. 2016). The compressive moduli of all the developed scaffolds with varied ratios have been illustrated in **Figure 4 (A).**

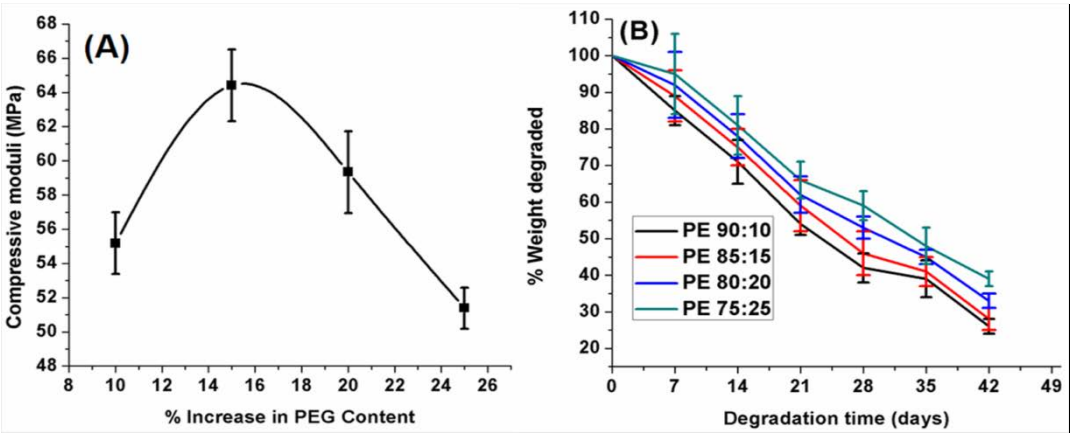

Figure 4: Compressive moduli (A) and degradation pattern (B) of PLA-PEG composite scaffolds. All the values are represented in Mean±SD (n=3).

In-vitro Biodegradation

The degradation rate of a scaffold is vital for restoring the entire tissue structure, both in-vitro and in-vivo (Siddiqui and Pramanik 2015). The obtained trend in the degradation property of the scaffolds is shown in **Figure 4 (B).** The minimal degradation rate is achieved with the sample (PE85:15) as it degraded only 28% of its original weight. The other composite scaffolds with different weight ratios of PEG have degraded as follows: PE90:10 (26%), PE80:20 (33%), and PE75:25 (39%). The difference in the degradation rate of PEG composite scaffolds attributed to the hydrophilic nature of PEG, which enhances the degradation of composite scaffolds. It is inferred that the addition of PEG leads to accelerated degradation, and similar results were reported earlier (Serra et al. 2014).

Metabolic Activity and Cell Attachment

MTT assay was employed to check the metabolic activity of the cells seeded on composite scaffolds. The cell viability has been found to increase over a period, as shown in **Figure 5**. The PLA-PEG composite scaffolds exhibited good biocompatibility irrespective of PEG content. However, a slight increase in the metabolic activity of the seeded cells has been noticed as the concentration of PEG increased, which may have been attributed to the increase in the hydrophilic property of composite scaffolds. Thus it is established that PEG conjugation can increase cellular metabolic activity as reported earlier (Kutikov and Song 2015; Pramanik et al. 2015).

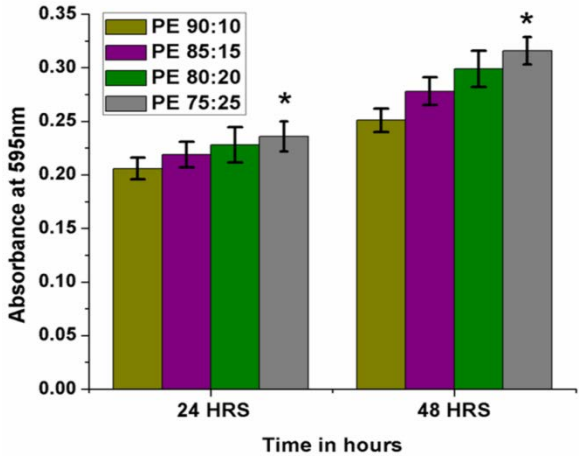

Figure 5: Metabolic activity of hMSCs on PLA-PEG composite scaffolds (PE 90:10; PE 85:15; PE 80:20 and PE 75:25) after 24 and 48 hr. All values represented in mean±SD (n=3). * indicates statistically significant difference at p>0.05.

Figure 6 A and B illustrates the cell attachment and spreading over PE90:10 and PE 75:25 scaffolds, respectively. It is evident from the figure that both the scaffolds supported the cells to attach, adhere, and spread. It was reported that PEG-based scaffolds provided ample support for cell adhesion, and the same was confirmed in our current investigation (Chen et al. 2008; Scaffaro et al. 2016; Tziampazis et al. 2000).

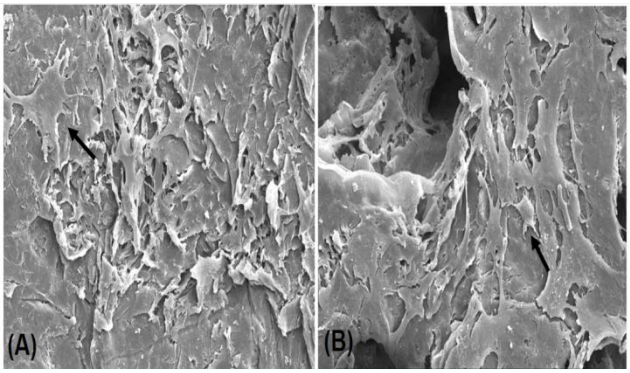

Figure 6: SEM images of cell attachment on PE 90:10 (A) and PE 75:25 (B) scaffold surface on day 3.

CONCLUSIONS

In the present work, solvent casting-particulate leaching was used to develop PLA-PEG composite porous scaffolds. These scaffolds have been characterized in detail for their physicochemical, mechanical, thermal, structural, and functional properties. In-vitro degradation studies of composite scaffolds showed an increase in degradation with increasing PEG concentration. The metabolic activity and cell attachment investigations confirmed that these scaffolds are cytocompatible. The composite scaffolds exhibited the porosity. The selected scaffolds were sterilized and cells were seeded to evaluate the cytocompatibility and cellular attachment property. Further studies on these scaffolds would bring the potential scaffolds for bone tissue engineering application.

Conflicts of Interest

The authors have no financial conflicts of interest

REFERENCES

1. Bissoyi A, Pramanik K (2013) Effects of non-toxic cryoprotective agents on the viability of cord blood derived MNCs. Cryo Letters 34 (5):453-465
2. Burg KJ, Porter S, Kellam JF (2000) Biomaterial developments for bone tissue engineering. Biomaterials 21 (23):2347-2359
3. Cai X, Tong H, Shen X, Chen W, Yan J, Hu J (2009) Preparation and characterization of homogeneous chitosan–polylactic acid/hydroxyapatite nanocomposite for bone tissue engineering and evaluation of its mechanical properties. Acta Biomater 5 (7):2693-2703
4. Causa F, Netti P, Ambrosio L, Ciapetti G, Baldini N, Pagani S, Martini D, Giunti A (2006) Poly-ϵ-caprolactone/hydroxyapatite composites for bone regeneration: In vitro characterization and human osteoblast response. J Biomed Mater Res Part A 76 (1):151-162
5. Chen BY, Jing X, Mi HY, Zhao H, Zhang WH, Peng XF, Turng LS (2015) Fabrication of polylactic acid/polyethylene glycol (PLA/PEG) porous scaffold by supercritical CO2 foaming and particle leaching. Polym Eng Sci 55 (6):1339-1348
6. Chen H, Yuan L, Song W, Wu Z, Li D (2008) Biocompatible polymer materials: role of protein–surface interactions. Prog. Polym. Sci. 33 (11):1059-1087
7. Chiu Y-C, Larson JC, Isom Jr A, Brey EM (2010) Generation of porous poly (ethylene glycol) hydrogels by salt leaching. Tiss Eng Part C: Methods 16 (5):905-912
8. Delaine-Smith RM, Green NH, Matcher SJ, MacNeil S, Reilly GC (2014) Monitoring fibrous scaffold guidance of three-dimensional collagen organisation using minimally-invasive second harmonic generation. PloS one 9 (2):e89761
9. George S (2001) Infrared and Raman characteristic group frequencies: tables and charts. Wiley, Chichester

10. Guelcher SA (2008) Biodegradable polyurethanes: synthesis and applications in regenerative medicine. Tiss Eng Part B: Reviews 14 (1):3-17
11. Jiang S, Liao G (2012) Synthesis and characterization of biocompatible poly (ethylene glycol)-b-poly (L-lactide) and study on their electrospun scaffolds. Polym Plast Technol Eng. 51 (12):1237-1244
12. Kokubo T, Kushitani H, Sakka S, Kitsugi T, Yamamuro T (1990) Solutions able to reproduce in vivo surface-structure changes in bioactive glass-ceramic A-W3. J Biomed Mater Res Part A 24 (6):721-734
13. Kumar Mekala N, Raju Baadhe R, Rao Parcha S (2013) Study on osteoblast like behavior of umbilical cord blood cells on various combinations of PLGA scaffolds prepared by salt fusion. Curr Stem Cell Res Ther 8 (3):253-259
14. Kutikov AB, Song J (2015) Biodegradable PEG-based amphiphilic block copolymers for tissue engineering applications. ACS Biomater Sci Eng. 1 (7):463-480
15. Liu D, Zhuang J, Shuai C, Peng S (2013) Mechanical properties' improvement of a tricalcium phosphate scaffold with poly-l-lactic acid in selective laser sintering. Biofabrication 5 (2):025005
16. Liu G-C, He Y-S, Zeng J-B, Xu Y, Wang Y-Z (2014) In situ formed crosslinked polyurethane toughened polylactide. Polym. Chem5)7:(2530-2539
17. Lu L, Mikos AG (1996) The importance of new processing techniques in tissue engineering. Mrs Bulletin 21 (11):28-32
18. Matsuura H, Miyazawa T, Machida K (1973) Infrared spectra of poly (ethylene glycol) dimethyl ethers in the crystalline state. Spectrochim. Acta Mol. Biomol. Spectrosc. 29 (5):771-779
19. Miyazawa T, Fukushima K, Ideguchi Y (1962) Molecular vibrations and structure of high polymers. III. Polarized infrared spectra, normal vibrations, and helical conformation of polyethylene glycol. TJ. Chem. Phys. 37 (12):2764-2776
20. Murphy WL, Dennis RG, Kileny JL, Mooney DJ (2002) Salt fusion: an approach to improve pore interconnectivity within tissue engineering scaffolds. Tiss Eng 8 (1):43-52
21. admanabhan A, Salvatore L, Gervaso F, Catalano M, Taurino A, Sannino A (2014) Synthesis and Characterization of Collagen Scaffolds Reinforced by Eggshell Derived Hydroxyapatite for Tissue Engineering-ResearchGate. J. Nanosci. Nanotechnol., United States of America:1-6
22. Place ES, Evans ND, Stevens MM (2009) Complexity in biomaterials for tissue engineering. Nat. Mater 8 (6):457
23. Pramanik S, Ataollahi F, Pingguan-Murphy B, Oshkour AA, Osman NAA (2015) In vitro study of surface modified poly (ethylene glycol)-impregnated sintered bovine bone scaffolds on human fibroblast cells. Scientific reports 5:9806
24. Rozenberg M, Loewenschuss A, Marcus Y (1998) IR spectra and hydration of short-chain polyethyleneglycols. Spectrochim. Acta Mol. Biomol. Spectrosc. 54 (12):1819-1826
25. Sah MK, Pramanik K (2014) Soluble-eggshell-membrane-protein-modified porous silk fibroin scaffolds with enhanced cell adhesion and proliferation properties. J. Appl. Polym. Sci. 131 (8)
26. Scaffaro R, Lopresti F, Botta L, Rigogliuso S, Ghersi G (2016) Preparation of three-layered porous PLA/PEG scaffold: relationship between morphology, mechanical behavior and cell permeability. J Mech Behav Biomed Mater 54:8-20
27. Serra T, Ortiz-Hernandez M, Engel E, Planell JA, Navarro M (2014) Relevance of PEG in PLA-based blends for tissue engineering 3D-printed scaffolds. Mater Sci Eng C 38:55-62
28. Siddiqui N, Pramanik K (2014) Effects of micro and nano β-TCP fillers in freeze-gelled chitosan scaffolds for bone tissue engineering. J. Appl. Polym. Sci 131 (21)
29. Siddiqui N, Pramanik K (2015) Development of fibrin conjugated chitosan/nano β-TCP composite scaffolds with improved cell supportive property for bone tissue regeneration. J. Appl. Polym. Sci. 132 (9)
30. Sultana N, Wang M (2012) PHBV/PLLA-based composite scaffolds fabricated using an emulsion freezing/freeze-drying technique for bone tissue engineering: surface modification and in vitro biological evaluation. Biofabrication 4 (1):015003
31. Tziampazis E, Kohn J, Moghe PV (2000) PEG-variant biomaterials as selectively adhesive protein templates: model surfaces for controlled cell adhesion and migration. Biomaterials 21 (5):511-520
32. Wang C, Feng L, Yang H, Xin G, Li W, Zheng J, Tian W, Li X (2012) Graphene oxide stabilized polyethylene glycol for heat storage. Phys. Chem. Chem. Phys. s 14 (38):13233-13238
33. Xu C, Inai R, Kotaki M, Ramakrishna S (2004) Aligned biodegradable nanofibrous structure: a potential scaffold for blood vessel engineering. Biomaterials 25 (5):877-886
34. Xu W, Ma J, Jabbari E (2010) Material properties and osteogenic differentiation of marrow stromal cells on fiber-reinforced laminated hydrogel nanocomposites. Acta biomater 6 (6):1992-2002
35. Yin H-M, Qian J, Zhang J, Lin Z-F, Li J-S, Xu J-Z, Li Z-M (2016) Engineering porous poly (lactic acid) scaffolds with high mechanical performance via a solid state extrusion/porogen leaching approach. Polymers 8 (6):213
36. Yu G, Ji J, Shen J (2006) Synthesis and characterization of cholesterol-poly (ethylene glycol)-poly (D, L-lactic acid) copolymers for promoting osteoblast attachment and proliferation. J. Mater. Sci. Mater. Med 17 (10):899-909
37. Zhu K, Xiangzhou L, Shilin Y (1990) Preparation, characterization, and properties of polylactide (PLA)–poly (ethylene glycol)(PEG) copolymers: a potential drug carrier. J. Appl. Polym. Sci 39 (1):1-9
38. Zhu X, Huang R, Zhong T, Wan A (2015) Striking dispersion of recrystallized poly (ethylene glycol)-poly (lactic acid) solvent-casting blend. arXiv preprint arXiv:150203060